

Excitation-energy transfer and metastable-particle desorption from electron-bombarded Xe films with N₂ and CO top layers

A. Mann,* P. Cloutier, D. Liu, and L. Sanche

Groupe du Conseil de Recherches Médicales en Sciences des Radiations, Faculté de Médecine, Université de Sherbrooke, Sherbrooke, Québec, Canada J1H 5N4

(Received 13 June 1994; revised manuscript received 10 November 1994)

We report experimental results on the desorption of metastable particles from N₂- and CO-covered solid Xe films induced by the impact of 6–26-eV electrons. The resemblance between the yield functions of the metastable particles and that of UV photons from a pure Xe film indicates that the desorption is a bulk-mediated process. We propose a mechanism for metastable-particle production based on a well-known gas-phase energy-transfer process between Xe* and N₂ (or CO): primary electrons create excitons which then transfer their energy to ground-state N₂ (or CO) molecules on the surface, producing metastable molecules, which can desorb.

I. INTRODUCTION

Recent experiments have shown that electronic excitations in rare-gas (RG) solids initiate secondary processes such as luminescence and particle desorption.^{1,2} The desorbed particles include rare-gas atoms themselves,^{2,3} surface-adsorbed atoms,^{1,2} and the fragments of the adsorbed molecules.⁴ In our experiments, low-energy electrons of 6–26 eV impinging on a RG solid create the primary excitations (i.e., an exciton or a hole). The primary excitations in the RG solid are mobile and known to evolve through two competitive channels:^{1–3} (a) direct radiative decay to the ground state, and (b) relaxation and localization which eventually leads to desorption or redshifted light emission. Distorted local environments like the surface, lattice imperfections, and impurity particles enhance the exciton (and the hole) trapping and localization. Surface-localized excitations are the precursor states for atomic and molecular desorption.

The formation and localization of surface excitons and their subsequent relaxation processes leading to desorption are especially sensitive to surface conditions and contaminations. Even experiments that concern only pure RG crystals have to consider the effect of possible contaminations from ambient gases. As early as in 1976, Ackermann *et al.*⁵ have observed that the quenching effect on the luminescence yield from Kr films was increasing with time due to surface contamination from the 10⁻⁹-mbar background. Since the desorption process is strongly correlated with the luminescence process, we also expect surface contamination to affect the desorption yields. The effects of impurities and their quenching mechanisms can be investigated by adding controlled amounts of “contaminants” like N₂ and CO into the bulk or onto the surface of RG crystals, in order to modify systematically the desorption and luminescence features.

Two types of energy transfer to adsorbates have been discussed previously:^{5,6} (i) diffusion of free excitons to the surface leading to “collisionally induced” energy transfer

to adsorbed particles, and (ii) energy transfer via dipole-dipole interaction from trapped excitons to adsorbants. The question of contamination-related quenching and trapping of excitons and holes has stimulated recent investigations of N₂- and O₂-doped Ar films, one observing the luminescence and total desorption yield⁷ and the other one studying the kinetic-energy spectra of desorbed Ar atoms.⁸ Our approach is in a way complementary since we are interested in new reaction channels opened only by adding the second species. We focus on the interaction which can lead to surface adsorbate desorption via lattice excitations. An example of such a process is the case of metastable xenon (Xe*) desorption from a multilayer Kr film covered by a monolayer of Xe.¹ The desorption is not observed with a comparable rate from either pure crystals. Two reaction channels are thought to lead to Xe* desorption: (i) the primary excitation of a Xe atom at a lattice site with Kr neighbors, and (ii) the excitation transfer from a bulk Kr exciton to a surface Xe atom. In both cases, the Xe* is ejected along a repulsive potential-energy surface.

In this paper, we describe and discuss similar experiments with N₂ and CO adsorbed onto Xe crystals. This substrate is chosen because it produces only UV photons under the bombardment of low-energy (<30 eV) electrons; no metastable particles (MP's) are observed by bombarding pure Xe solids.¹ However, we show that considerable MP desorption occurs from N₂- and CO-covered solid Xe films. From the energy analysis, we conclude that the detected particles are N₂* in the *A*³Σ_u⁺ and CO* in the *a*³Π metastable states. Comparison of the yield functions for the MP with those of the UV photons from a pure Xe film indicate that the desorption is a bulk-mediated process. We propose a mechanism for MP production based on a well-known gas-phase energy-transfer process between Xe* and ground-state N₂ (or CO): primary electrons create excitons which then transfer their energy to ground-state N₂ (or CO) molecules on the surface producing desorption of metastable diatomic molecules.

II. EXPERIMENT

The experimental arrangement has been described in detail previously.³ Briefly, a well-collimated electron beam produced by a 127° cylindrical monochromator impinges on a target consisting of a RG film having a thickness lying between 5 and 100 ML and a 1-ML diatomic overlayer. The target is condensed on a Pt(111) crystal held at 20 K under UHV conditions. The Pt crystal surface is cleaned by electrical heating with and without the presence of oxygen; its degree of crystallinity is measured by low-energy electron diffraction. The electron beam has a resolution of 60 meV full width at half maximum (FWHM) and its energy can be varied between 0.1 and 100 eV depending on the adjustment of the electron lenses. The electron energy with respect to the vacuum level is determined by measuring the onset of the target current as a function of the voltage applied between the Pt(111) crystal and the monochromator. The absolute electron energy scale is accurate within ± 0.3 eV.

UV luminescence and desorbing MP's are detected with a large area (45 cm²) microchannel plate (MCP) array; the MCP array is superimposed on a position-sensitive anode for current measurement with angular resolution. Grids in front of the MCP, which are successively biased positively and negatively, repel all charged particles. The use of a pulsed electron beam allows us to measure time-of-flight spectra and restrict the origin of counted events when recording yield functions. With pulse durations of about 10 μ s chosen for the present experiments, the time-of-flight signal provides a discrimination between photons and heavy metastable particles while providing the velocity distribution of the latter. The path length (d) between the target and the MCP is 5.2 ± 0.1 cm. This parameter is related to the energy $E(t)$ of the MP's by the relation

$$E(t) = \frac{M}{2} \left[\frac{d}{t} \right]^2, \quad (1)$$

where M is the mass of the MP (28 amu for N₂ and CO) and t is the time of flight. From this relation, we find

$$\Delta E(t) = \frac{Md}{t^2} \left[\Delta d + \frac{d}{t} \Delta t \right] \quad (2)$$

for the resolution in translational energy of the MP's. Using $\Delta t = 5 \mu$ s we calculate $\pm 11\%$ at 20 meV and $\pm 25\%$ at 200 meV. As we shall see, this resolution is further decreased by the noise level at low energies. With the present electron-beam intensity ($j \leq 1$ nA/mm²; $E \leq 30$ eV), we can neglect the interactions between electron-beam induced excitations in the target. This condition is corroborated by the shape of the yield functions for Kr and Xe excitons.¹

The features of the MCP are relevant in the present context and deserve a short discussion. We use a pile of three standard MCP's (Galileo) with an Inconel metallic coating facing the sample. According to the manufacturer, the UV detection efficiency without a high-yield photocathode coating lies around 5–10 % for photon energies above of 10 eV and drops by about three orders mag-

nitude for 8-eV photons. The low secondary-electron emission coefficient for photons is due to their weak interaction with the bulk which results in a rather large penetration depth. On average, the electrons will be excited far away from the MCP surface and only a small fraction of them will be able to leave the bulk and start an electron cascade. On the other hand, an incoming metastable-particle transfers its excitation energy via an Auger-type process to a single electron close to the surface. Thus, the efficiency should be high if the transferable energy exceeds the local work function (metal electrode or lead glass inside a channel, both covered by background molecules). We expect that the excitation energy released in the Auger process is determined by the Franck-Condon factors for transitions between the metastable state and different vibrational levels of the ground state. Consequently, a threshold for MP detection cannot be given unambiguously, but as a reference value we mention a recent experiment detecting CO (*a*³Π) with a 0-0-transition energy of 6.01 eV.⁹ Above this threshold, we also expect some variations of the sensitivity of the MCP depending on the transferable internal energy of the MP. For the N₂^{*} and CO^{*} states measured in the present experiment, these variations should be small since both states have about the same internal energy and Franck-Condon factors to the ground state when they strike the detector. However, the relative magnitudes of the signals between N₂^{*} and CO^{*} are affected by variations in the experimental conditions between different experiments resulting in an estimated error of 20% for reproducing the intensities.

III. RESULTS

Considerable signal due to metastable nitrogen-molecule (N₂^{*}) desorption is observed in the case of a N₂ ML on top of a 50-ML Xe film [Fig. 1(a)]. The yield function of the N₂^{*} [Fig. 1(a)] shows only broad features compared to the energy resolution of the incident electron beam. The threshold at ~ 7.0 eV is followed by a peak with its maximum at 9.8 eV and a FWHM of about 3 eV. The MP yield increases again with energy starting from 15 eV and reaches a plateau at 22 eV. The shape of the yield function for N₂^{*} resembles very much that for UV luminescence from the pure Xe film, which is given for comparison in Fig. 1(b). The MP and UV-photon yields have very similar energy thresholds and peak features. Shown in Fig. 2 is the time-of-flight data for 1 ML of N₂ condensed on 50 ML of Xe (thereafter referred to as 1N₂/50Xe) recorded with 10- and 25-eV electron beams. Both spectra have the same vertical gain and exhibit the same time-of-flight profile. The curve in the inset represents the kinetic energy spectrum of the MP's obtained by transforming curve (*a*) using Eq. (1). The maximum in the energy distribution appears to lie around 20 meV (i.e., within the error limit). In such spectra, the noise level increases drastically at lower energies due to diminishing signal-to-noise ratio with increasing flight times. The vertical arrow in the inset points to the energy of the peak in (*a*).

The interpretation of the MP signal as due to N₂^{*} is

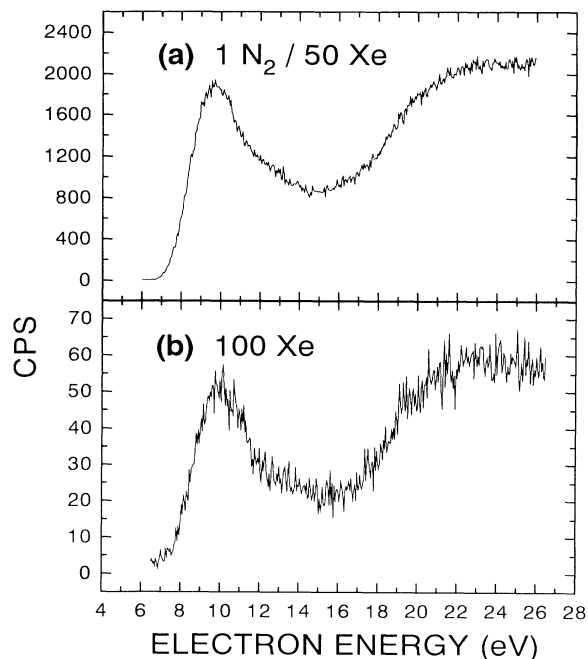


FIG. 1. (a) Yield function of metastable-particle desorption from a 50-ML Xe(111) film covered by a monolayer of N_2 ; and (b) excitation function of the luminescence signal from a 100-ML Xe(111) film.

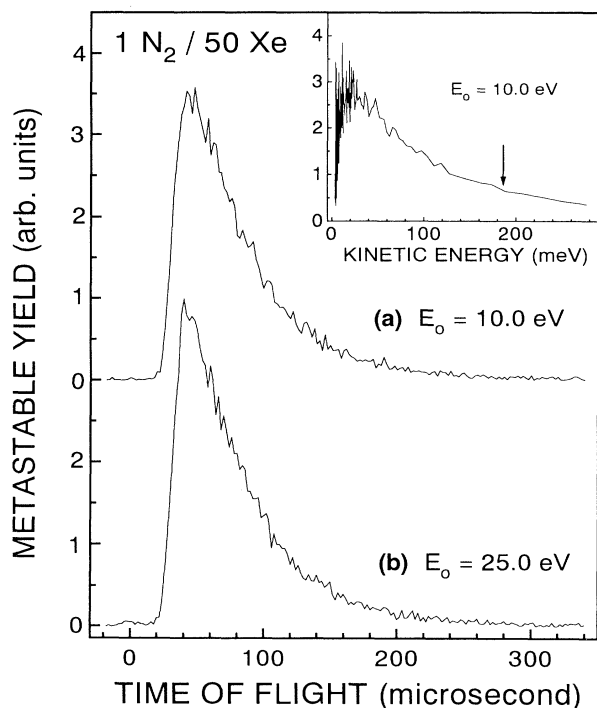


FIG. 2. Time-of-flight (TOF) data for metastable particles desorbed by (a) 10-eV and (b) 25-eV electrons from one ML of N_2 adsorbed on 50 ML of Xe (i.e., a 1 N_2 /50 Xe film). The energy distribution of the metastable particles desorbed by 10-eV electrons is shown in the inset. The position of the vertical arrow corresponds to the maximum in the TOF spectrum.

based on the elimination of other possible candidates, Xe^* and N^* . It has been shown before¹ that Xe^* atoms do not desorb from a pure Xe film under our experimental conditions. Considering N^* , any such species would involve the dissociation of a N_2^* state having an energy higher than 16 eV since the lowest dissociation limit is close to 10 eV and the internal energy of the fragment must be at least 6 eV.¹⁰ As shown in Fig. 1(a), the actual energy threshold for the MP desorption is at about 7 eV. For N_2 there are a number of metastable states that are sufficiently low in energy to match the threshold of the excitation function and possess sufficient internal energy to trigger a signal at the MCP detector (e.g., $A^3\Sigma_u^+$, $B^3\Pi_g$, $W^3\Delta_u$, $a^1\Pi_g$, ...).¹⁰ Furthermore, any N^* species would be the product of N_2 dissociation along step potential-energy curves leading to the formation of MP with eV's of energy. These energies couple with the lower mass for N would produce a MP signal at times shorter than 20 μs in the time-of-flight (TOF) spectra. This would be inconsistent with the results of Fig. 2.

For a CO ML on top of Xe film, the signal observed at the MCP detector is approximately an order of magnitude weaker than that for N_2 . Figure 3 shows the MP signal from a 1-ML CO/50-ML Xe film; the line shape of its energy dependence is similar to the above-mentioned yield function for N_2 /Xe. As in the case of N_2 , interpretation of the signal in Fig. 3 as due to metastable carbon monoxide (CO^*) is dictated by the elimination of the other possibilities.¹¹ The time-of-flight data for MP's from 1CO/50Xe bombarded with 10- and 23-eV electrons are shown in Fig. 4 and the energy spectrum displayed in the inset. Again, both curves have the same time-of-flight profile. Within the present resolution, the TOF and energy spectra in Figs. 2 and 4 must be considered similar indicating that the metastable N_2^* molecules have on the average about the same kinetic energy as that of the CO^* molecules. Further experiments show that the TOF peak positions do not depend on the electron-beam energy within the present energy range. We have also studied the dependence of the N_2^* and CO^* yields on the thickness of the Xe film for a single-layer diatomic adsorbate. Both yields increase with thickness up to about 10 ML of Xe.¹²

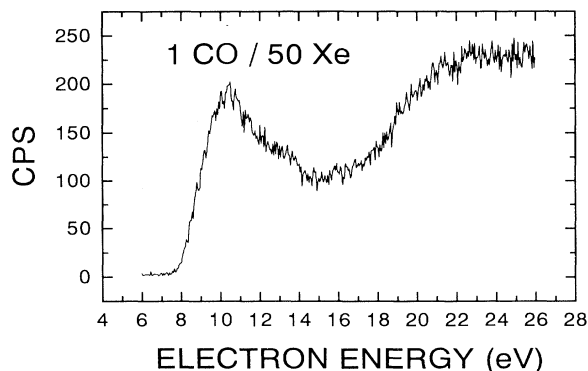


FIG. 3. Yield function of metastable-particle desorption from a 50-ML Xe(111) film with a monolayer coverage of CO.

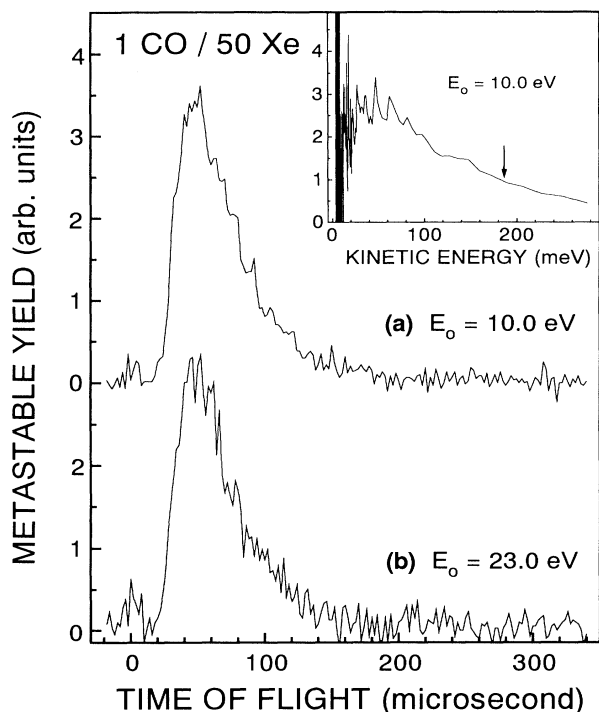


FIG. 4. TOF data for metastable particles desorbed by (a) 10-eV and (b) 23-eV electrons from a 1 CO/50 Xe film. The energy distribution of the metastable particles desorbed by 10-eV electrons is shown in the inset. The position of the vertical arrow corresponds to the maximum in the TOF spectrum.

IV. DISCUSSION

Both N_2 and CO are physisorbed on the RG surfaces with an estimated binding energy of less than 200 meV.¹³ The interaction is of van der Waals type and thus the molecules are expected to be lying flat on the surface in order to minimize the average distance. The CO molecule should bind stronger to the surface because of its higher polarizability and permanent dipole moment. A herringbone in-plane structure has been proposed for $N_2/Xe/Ag(111)$ (Ref. 14) as well as for $N_2/graphite CO/Ag(111)$.¹⁵

First, it should be noted that CO^* desorption from CO chemisorbed on Pt(111) has been observed in electron-stimulated desorption (ESD) experiments with electron energies of about 200 eV.⁹ Since CO is chemically bound to the Pt (terminal or bridge site) in this case, bond breaking by interaction with primary electrons is the basic desorption mechanism. However, with a RG layer placed between the CO layer and the Pt crystal (as in our experiment), the character of adsorption changes from chemical to physical and the CO^* desorption processes become different.

A successful model for MP desorption from RG solids is the "cavity expulsion" mechanism introduced at first for Ar crystals.¹⁶ The excited atom or molecule located at the surface (as a trapped exciton) experiences a slightly repulsive interaction with all neighbors and this repulsive

potential propels the excited species into vacuum. Inside the bulk, this repulsion would lead to a cavity around the excited particle. Quantitative calculations¹⁷ were able to predict details of the Ar^* desorption³ and the absence of cavity expulsion of Kr^* from Kr crystals. A propensity rule states that in RG crystals with negative- (positive-) electron affinity the excited particle is (is not) expelled owing to the repulsive (attractive) interaction of the excited-orbit electron cloud with the neighboring atoms. In our case with a two-layer N_2/Xe system, neither calculations nor estimates concerning the fate of a N_2^* or a CO^* in the surface layer are available. However, the question to address in the first place dealing with mixed-species films is the following: How can we describe a process starting with a low-energy electron which leads to a localized excitation at a particular adsorbed particle?

As shown in Fig. 1, the yield function for N_2^* from $1N_2/50Xe$ tracks that for UV photons from a pure 100-ML Xe film. The resemblance in the two yield functions and the Xe thickness dependence of the N_2^* yield indicate that MP desorption is a bulk-mediated process. Bulk excitons are able to carry the initial excitation energy to the surface. In order to determine the reaction path from a Xe bulk exciton to a desorbing N_2^* , a comparison with gas-phase results on the excitation transfer in $Xe^* + N_2$ reactions is helpful. Experimental results^{18,19} have been reported on low-energy collisions of metastable Xe ($^3P_{2,0}$) and ground state N_2 ($X^1\Sigma_g^+$) with state selective detection of the excited N_2 . Due to spin conservation, N_2 is excited into the triplet manifold, and the patterns of radiative decay within that system give clear evidence that the N_2 state produced in the collisions is almost exclusively $B^3\Pi_g$ in a small range of vibrational levels around the resonance energy. A potential energy picture is successfully applied to explain the observed distribution of N_2 states after Xe (3P) impact.²⁰ The potential-energy curves are constructed from a number of experimental results on the Xe- N_2^* system. In the exit channel, one has a set of curves, each containing an additive constant given by the respective vibrational level. These curves are generally quite flat in the outer region ($r > 3.5-4 \text{ \AA}$) and rather steep and repulsive for smaller distances. In the entrance channel, due to the large radius of the Xe 6s orbital, the interaction is starting at larger distance ($r = 4-4.5 \text{ \AA}$) and some branches show local minima. The reaction proceeds via curve crossings and is exoergic or slightly endoergic.

A similar gas-phase reaction^{19,21} for CO and Xe ($^3P_{0,2}$) produces initial excitation of the $a'^3\Sigma^+$ and $d^3\Delta$ states in the collision. Both excited states then decay to the metastable $a^3\Pi$ state. The overlap of the wave functions of upper and lower state determines that only little energy is kept as vibrational energy in the a state, even if there is a larger amount of it in the a' and d states. The vibrational populations for energy transfer from Xe ($^3P_{0,2}$) to N_2 and CO molecules are given in Table I.

At higher collision energy, CO and N_2 show different reaction behavior. Elevated kinetic energy of the scattering particles results in a higher vibrational excitation of the $CO(a',d)$ product. The cross section for the higher

TABLE I. Vibrational levels of excited N₂ (CO) states populated after gas-phase collision of the respective ground-state molecule with Xe (³P_{0,2}). Only substantially populated levels are listed. The levels of the first state of every pair [N₂ (*B*), CO (*a'*), and CO (*d*)] are determined by the collision process and always near-resonant, while the second state [N₂ (*A*), CO (*a*)] is reached after radiative decay of the former (Franck-Condon transitions).

Vibrational levels	Xe (³ P ₂)	Xe (³ P ₀)
N ₂ (<i>B</i> ³ Π _g)	5 ^a	10–11 ^a
N ₂ (<i>A</i> ³ Σ _u ⁺)	2–3 ^a	6–8 ^{a,b}
CO (<i>a'</i> ³ Σ _u ⁺)	11 ^a	20–21
CO (<i>a</i> ³ Π)	0–1 ^{a,b}	2–3 ^b
CO (<i>d</i> ³ Δ)	6 ^a	15–16
CO (<i>a</i> ³ Π)	0–1 ^{a,b}	2–3 ^b

^aFrom Ref. 19.

^bCalculated (as transition probabilities) using RKR potentials [N₂ (Ref. 27), CO (Refs. 28 and 29)].

vibrational excitation increases with kinetic energy. In contrast for N₂, the increased scattering energy does not result in a higher vibrational excitation of the N₂ (*B*) product. It follows that the kinetic energy after the collision is higher for N₂ than for CO excited molecules.

In analogy to these gas-phase results, we are tempted to consider an energy transfer from the Xe substrate to the diatomic molecule as a result of a “collision” between a Xe exciton and an adsorbed molecule *M* on the film surface. The energy values of the excited states of the molecular adsorbates are only slightly changed from gas phase to (physisorbed) condensed phase [see Ref. 22 for N₂ and CO] and the lowest bulk exciton energy for Xe is 60 meV higher than the respective ³P₂ energy. Thus, an excitation transfer similar to the gas phase is proposed for the metastable-molecular desorption in the bilayer film. Within this model, the process at the film surface is seen as a “half-collision process” since there is no nuclear motion of the reaction partners in the incoming channel. The starting point of this half-collision process is the excited complex RG*–*M* at the surface with the nuclei at their ground-state distance. At this point, the bulk exciton of energy *E*_{ex} becomes localized around the RG atom due to a distorted environment. The electronic energy transfer from the surface exciton to the adjacent adsorbed molecule (either N₂ or CO) via potential-energy curve crossing changes the excited complex to RG–*M**. The excess energy available after the energy-transfer reaction is

$$E_0 = E_{\text{ex}} - E(n, v, j), \quad (3)$$

where *n*, *v*, and *j* represent electronic, vibrational, and rotational (or librational) quantum numbers of the energy state *E* of the surface molecule. If *E*₀ exceeds the binding energy *D*_c of *M**, desorption is energetically possible, but in order to comply with momentum conservation, a number of phonons have to be created (or absorbed) in the process. The relations for energy and momentum conservation for a molecule *M* desorbing with momentum *p* and mass *m* are written as

$$E_0 - D_c = \frac{p_M^2}{2m} \pm \sum_i \hbar\omega(\mathbf{k}_i), \quad (4)$$

$$0 = p_M \pm \sum_i \hbar\mathbf{k}_i \pm \hbar\mathbf{K}, \quad (5)$$

where *k_i* is the wave vector of the *i*th phonon and *K* is a reciprocal lattice vector. The wave vector of the exciton is neglected. The kinetic energy of the desorbing molecule is therefore a question of intramolecular vibrational excitation and phonon statistics. Shortly, a bulk exciton diffusing to a surface Xe atom places the Xe-molecule system into the starting position of the half-collision process. Along with the excitation transfer the molecule separates away from the Xe atom on a particular exit-potential-energy surface. If the molecule gains sufficient kinetic energy to overcome the physical binding barrier [i.e., if $E_0 \pm \sum_i \hbar\omega(\mathbf{k}_i) > D_c$], it desorbs.

The previously mentioned gas-phase studies can be used to explain the yield difference between N₂ and CO in our experiments. According to Eqs. (3)–(5), molecules which populate the highest vibrational level [i.e., having large $E(n, v, j)$] will gain less kinetic energy from the reaction. If the kinetic-energy term in Eq. (4) is negative, the molecule cannot directly desorb from the surface. According to Table I, the CO molecules are created at the surface with more vibrational energy than N₂ molecules. Moreover, the slight increase in the anisotropy of the intermediate excited state (i.e., RG–*M**) for CO, due to its permanent dipole moment, could partition more energy into rotational states and further reduce the energy available for translational motion in comparison to N₂. This energy partitioning could be responsible for the CO* yield being about 1 order of magnitude smaller than the N₂* yield as shown in Figs. 1 and 3.

The vibrationally excited adsorbates that cannot surpass the energy barrier in the first step, have another option for desorption: bond rupture through energy transfer from the internal vibrational excitation of the molecule to the adsorbate-surface bond. If the adsorbed molecule is in a vibrational energy level which is degenerate with some continuum state of the surface-molecule bond, cross over into the latter state will lead to desorption of the molecule in a lower vibrational level. The feasibility of this mechanism has been demonstrated experimentally and theoretically.^{23–26} In our case, the molecules on the surface are initially excited to high vibrational levels of the metastable electronic states (Table I). Assuming that the radiative decay on the surface of our films is similar to the gas-phase processes, the lifetime of the N₂ (*B*) state [4–8 μs (Ref. 27)] is more than six orders of magnitude larger than the periods of intramolecular vibrations and molecule-surface modes. It is therefore sufficiently long to allow desorption via transfer of vibrational energy to molecule-surface modes.²⁵ According to the flight time in Fig. 2, the *B* state decays to the metastable *A* ³Σ_u⁺ state on its way to the detector. For CO, radiative decay lifetimes of the *a'* and *d* states in the order of 3 μs (Ref. 29) and 5 μs,^{21,30} respectively, also allow sufficient time for the energy transfer. Essentially CO (*a*) will be detected in this case.

However, there are other competing energy-transfer processes in the condensed phase that reduce the initial vibrational populations. In a N_2 -doped Xe solid, the deexcitation of excited-state vibrational energy is possible either directly in $\Delta v=1$ steps as multiphonon emitting process or indirectly in $\Delta v=2$ steps by exchange interaction with a ground-state molecule at a neighboring site, e.g., $N_2(A, v) + N_2(X, v') \rightarrow N_2(A, v-2) + N_2(X, v'+2)$,³¹ and releasing less energy to phonon modes. For a closely packed surface layer the latter process is expected to be fast compared to the electronic deexcitation. Generally, this reaction is important for molecules and states if it is quasisonant in energy, as for CO ($a', d-X$) in contrast to N_2 ($B-X$).²⁹ The higher rate for relaxation by exchange presumably leads in terms of the bond-rupture model to a lower desorption yield. Thus, this energy-transfer process again tends to decrease the CO^* desorption yield compared to N_2^* and appears to be consistent with our observation.

Finally we note that, although excitation-energy transfer from solid Xe to an adsorbate molecule appears as the dominant mechanism leading to MP desorption, it is not necessarily the only one. Direct electronic excitation of the adsorbate by incident electrons could also propel N_2^* in vacuum by cavity expulsion.¹⁶ As mentioned previously, this mechanism is usually not expected to be operative on a surface having a positive-electron affinity, but it is quite probable, however, that our "single" diatomic layer presents imperfections where clustering and double layering occurs. At those imperfections MP emission in vacuum would occur near diatomic neighbors where cavity expulsion may be more favorable. In fact, recent experiments¹² performed with the present apparatus indicate that appreciable N_2^* and CO^* yields are produced by 6–26-eV electrons impinging on multilayer N_2 and CO films, respectively. The N_2^* production starts at 7.0 eV whereas the threshold for CO^* is only observed around 8.5 eV. A close look at the MP yield functions in Figs. 1 and 3 reveals that the threshold for N_2^* lies about

0.6 eV below that for CO^* desorption. This difference may be due to the different energy thresholds for producing N_2^* and CO^* . Since below 8 eV Xe^* production is weak, the N_2 signal below that energy may be (at least partly) due to the cavity-expulsion mechanism. According to the CO multilayer results¹² such a signal should be completely absent below 8.5 eV in the present data.

V. CONCLUSION

We have found that desorption of metastable N_2^* and CO^* molecules is induced by the impact of 6–26-eV electrons on single layers of N_2 and CO, respectively, condensed on Xe substrates. These results and earlier ones on the Xe/Kr system,¹ as well as those of a study on negative-ion desorption from H_2O , C_2D_6 , and C_6D_6 adsorbed onto RG films,⁴ have shown that the RG films are very effective as a buffer for the excitation-energy transfer to adsorbants. In all above-mentioned systems the metastable particle signal is increasing with the thickness of the RG film, up to the penetration depth of electrons and excitons. Desorption due to interaction of RG bulk excitations and surface molecules is much stronger than desorption due to direct interaction of primary electrons with molecules in the surface layer. Based on our observations, we propose the following physical picture for the desorption of metastable species from atoms and molecules physisorbed on RG substrates: (i) the primary electron beam creates excitons in the RG film, (ii) excitons diffuse within the film modifying the initial energy deposition distribution, and (iii) the excitons created on or diffused to the surface transfer their energy to the surface molecules leading to desorption of metastable molecules.

ACKNOWLEDGMENTS

The authors wish to thank Dr. Michael Huels for helpful comments. This work was sponsored by the Medical Research Council of Canada.

*Present address: Hauptstrasse 9, 55599, Eckelsheim, Germany.

¹A. Mann, G. Leclerc, and L. Sanche, Phys. Rev. B **46**, 9683 (1992).

²P. Feulner and D. Menzel, in *Laser Spectroscopy and Photochemistry on Metal Surfaces*, edited by H.-L. Dai and W. Ho (World Scientific, Singapore, in press).

³G. Leclerc, A. D. Bass, A. Mann, and L. Sanche, Phys. Rev. B **46**, 4865 (1992).

⁴P. Rowntree, L. Parenteau, and L. Sanche, Chem. Phys. Lett. **182**, 479 (1991); P. Rowntree, H. Sambe, L. Parenteau, and L. Sanche, Phys. Rev. B **47**, 4537 (1993).

⁵Ch. Ackermann, R. Brodmann, U. Hahn, A. Suzuki, and G. Zimmerer, Phys. Status Solidi B **74**, 579 (1976).

⁶N. Schwentner, E.-E. Koch, and J. Jortner, *Electronic Excitations in Condensed Rare Gases* (Springer, Berlin, 1985).

⁷C. T. Reimann, W. L. Brown, and R. E. Johnson, Phys. Rev. B **37**, 1455 (1988).

⁸E. Hudel, E. Steinacker, and P. Feulner, Phys. Rev. B **44**, 8972 (1991).

⁹A. Szabó and J. T. Yates, Jr., J. Chem. Phys. **98**, 689 (1993), and references therein.

¹⁰H. H. Michels, Adv. Chem. Phys. **45**, 225 (1981).

¹¹G. Herzberg, *Spectra of Diatomic Molecules* (Van Nostrand Reinhold, New York, 1950), p. 452.

¹²H. Shi, P. Cloutier, and L. Sanche (unpublished).

¹³Ph. Avouris, D. Schmeisser, and J. E. Demuth, J. Chem. Phys. **79**, 488 (1983).

¹⁴M. Bertolo, W. Hansen, and K. Jacobi, Phys. Rev. Lett. **67**, 1898 (1991).

¹⁵D. Schmeisser, F. Greuter, E. W. Plummer, and H.-J. Freund, Phys. Rev. Lett. **54**, 2095 (1985).

¹⁶F. Coletti, J. M. Debever, and G. Zimmer, J. Phys. (Paris) Lett. **45**, 467 (1984).

¹⁷S. Cui, R. E. Johnson, and P. T. Cummings, Phys. Rev. B **39**, 9580 (1989); W. T. Buller and R. E. Johnson, *ibid.* **43**, 6118 (1991).

¹⁸N. Sadeghi and D. W. Setser, Chem. Phys. Lett. **82**, 44 (1981).

¹⁹T. Krümpelmann and Ch. Ottinger, Chem. Phys. Lett. **140**,

- 142 (1987).
- ²⁰V. Aquilanti, R. Candori, F. Pirani, T. Krüpelmann, and Ch. Ottinger, *Chem. Phys.* **142**, 47 (1990).
- ²¹M. Tsuji, K. Yamaguchi, and Y. Nishimura, *Chem. Phys.* **125**, 337 (1988).
- ²²R. M. Marsolais, M. Michaud, and L. Sanche, *Phys. Rev. A* **35**, 607 (1987).
- ²³Z. W. Gortel, H. J. Kreuzer, P. Piercy, and R. Teshima, *Phys. Rev. B* **27**, 5006 (1983).
- ²⁴I. Hussla, H. Seki, T. J. Chuang, Z. W. Gortel, H. J. Kreuzer, and P. Piercy, *Phys. Rev. B* **32**, 3489 (1985).
- ²⁵B. Fain and S. H. Lin, *Chem. Phys. Lett.* **114**, 497 (1985).
- ²⁶B. Fain, *Chem. Phys. Lett.* **118**, 283 (1985).
- ²⁷A. Lofthus and P. H. Krupenies, *J. Phys. Chem. Ref. Data* **6**, 113 (1977).
- ²⁸S. G. Tilford and J. D. Simmons, *J. Phys. Chem. Ref. Data* **1**, 147 (1972).
- ²⁹K. P. Huber and G. Herzberg, *Molecular Spectra and Molecular Structure* (Van Nostrand Reinhold, New York, 1979), Vol. 4.
- ³⁰T. G. Slanger and G. Black, *J. Phys. B* **5**, 1988 (1972).
- ³¹D. Kuszner and N. Schwentner, *J. Chem. Phys.* **98**, 6965 (1993).